SLAC-PUB-8912
July 2001

INDUCED RADIOACTIVITY OF MATERIALS BY STRAY RADIATION FIELDS AT AN ELECTRON ACCELERATOR *

S. H. Rokni, T. Gwise, J. C. Liu, S. Roesler
Stanford Linear Accelerator Center, Stanford University, Stanford, California 94309
A. Fassò
CERN-EP / AIP, CH-1211 Geneva 23, Switzerland

Abstract

Samples of soil, water, aluminum, copper and iron were irradiated in the stray radiation field generated by the interaction of a 28.5 GeV electron beam in a copper-dump in the Beam Dump East facility at SLAC. The specific activity induced in the samples was measured by gamma spectroscopy and other techniques. In addition, the isotope production in the samples was calculated with detailed Monte Carlo simulations using the FLUKA code. The calculated activities are compared to the experimental values and differences are discussed.

*Work supported by Department of Energy contract DE-AC03-76SF00515

Induced Radioactivity of Materials by Stray Radiation Fields at an Electron Accelerator

S. H. Rokni, [a] A. Fassò, [b] T. Gwise, [a] J. C. Liu, [a] S. Roesler [a]

[a] *Stanford Linear Accelerator Center, MS. 48, 2575 Sand Hill Road, Menlo Park, California 94025, USA*
Tel.: +1-650-926-2048, Fax: +1-650-926-3569
Email: rokni@slac.stanford.edu

[b] *CERN-EP/AIP, CH-1211 Geneva 23, Switzerland*

Abstract

Samples of soil, water, aluminum, copper and iron were irradiated in the stray radiation field generated by the interaction of a 28.5 GeV electron beam in a copper-dump in the Beam Dump East facility at SLAC. The specific activity induced in the samples was measured by gamma spectroscopy and other techniques. In addition, the isotope production in the samples was calculated with detailed Monte Carlo simulations using the FLUKA code. The calculated activities are compared to the experimental values and differences are discussed.

Key words: Induced radioactivity, Stray radiation fields, Photonuclear reactions, FLUKA

1 Introduction

One of the main radiation safety issues at high-energy electron accelerators is the personnel exposure from induced radioactivity in beam line components and shielding materials. Additionally, the concentration of induced activity in the groundwater and soil in the environment surrounding the accelerator needs to be carefully evaluated as part of documents required by overseeing agencies. Therefore, an accurate calculation of the induced radioactivity in various materials has become an essential part of the design and operation of high-energy electron accelerators.

The radiation field causing induced radioactivity at electron accelerators is very complex as it involves both electromagnetic and hadronic cascade processes. Calculation techniques based on analytical methods that are commonly

used in predicting the amount of induced activity have generally large uncertainties associated with them [1]. These uncertainties can be at least an order of magnitude [2], for example in situations where multi-material structures are exposed to beam or stray radiation. Additionally, analytical methods require information on production cross sections of various radionuclides which often does not exist.

Recently, the Monte Carlo particle interaction and transport code FLUKA [3–5] has been used in calculating directly the isotope production by electron-induced particle showers [2,6,7]. In order to estimate the reliability and predictive power of the involved models the results have to be benchmarked against experimental data. Unfortunately, such experimental information is still very limited for electron accelerators. A first detailed benchmark study based on an in-beam geometry experiment [8] was discussed in [2]. However, radioactivity in an accelerator environment is often caused by stray radiation which may activate beamline components, cooling water circuits as well as in soil and groundwater. A benchmark study of this aspect can be found in [6] which, however, carried large uncertainties associated with the number of beam particles, the chemical composition of the samples used in the measurement and the correction for self-absorption due to the thickness of the targets.

In order to provide further data on activation of materials by stray radiation fields an experiment was performed in the Beam Dump East facility at the Stanford Linear Accelerator Center. Samples of soil, water, aluminum, copper and iron were exposed to stray radiation from the interaction of 28.5 GeV electrons in a beam dump. This paper describes the measurements and data analysis and compares the specific activities of the different samples with results of detailed FLUKA calculations.

2 The Experiment

The soil sample was taken from an area on the SLAC site and its stones and other debris were removed. It was dried, sieved to 0.208 mm and packaged in a 500 ml plastic-bottle. An outside company[1] determined the chemical composition which is listed in Table 1 using a combination of Proton Induced X-ray Emission (PIXE), Proton Induced Gamma-ray Emission (PIGE) and Fast Neutron Activation Analysis techniques. The density of the soil sample was measured to be 1.3 g/cm^3. Furthermore, a sample of Low Conductivity Water was prepared by filling it also into a 500 ml bottle.

The metallic samples had a diameter of 4.45 cm and a thickness, density, and

[1] Element Analysis Corporation, 101 Ventura Ct., Lexington, KY 40510

Table 1
Chemical composition of the soil sample (in percent by weight).

O	54.41	Mn	3.163×10^{-2}
Si	31.98	Zr	1.987×10^{-2}
Al	6.235	Sr	9.705×10^{-3}
Fe	2.106	Ni	6.684×10^{-3}
Na	1.841	Cu	5.108×10^{-3}
K	1.219	Zn	4.694×10^{-3}
Mg	1.045	Rb	4.439×10^{-3}
Ca	6.782×10^{-1}	Pb	2.440×10^{-3}
Ti	3.495×10^{-1}	Br	7.931×10^{-4}
Cr	5.034×10^{-2}	Ga	5.969×10^{-4}

composition as given in Table 2. The iron sample was taken from the stock

Table 2
Density, thickness, and chemical composition (in percent by weight) of the metallic samples.

Sample	Iron		Aluminum		Copper	
Density (g/cm^3)	7.43		2.67		8.89	
Thickness (mm)	0.9		0.7		1.6	
Composition (%)	Fe	99.15	Al	99.82	Cu	99.415
	Sn	0.5	Fe	0.18	Zn	0.5
	Mn	0.35			Sn	0.05
					Ni	0.025
					Ag	0.01

that is used for building magnets at SLAC. The composition of the metallic samples was again determined by an outside company [2] using chemical analysis methods.

For the experiment a water-cooled copper dump, 14.4 cm in diameter and 25.2 cm in length, was placed in the Beam Dump East facility upstream of the main beam dump D400. The metallic disks were taped on the soil and water bottles which were placed on an aluminum table 31 cm below the dump. The irradiation started on February 6, 2000 and lasted for about 3 days during

[2] Calcoast Analytical, 4072 Watts Street, Emeryville, CA 94608

which a total of 2.88×10^{16} beam electrons of an energy of 28.5 GeV were sent onto the dump. The irradiation profile was monitored with an upstream toroid and is shown in Fig. 1.

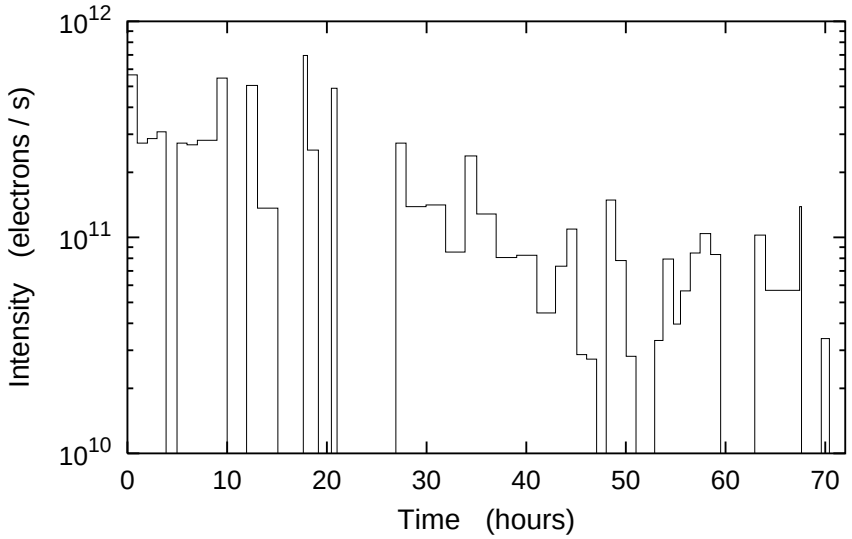

Fig. 1. Beam profile during the experiment.

3 Data Analysis

3.1 Tritium Measurements

A liquid scintillation counter [3] was used to analyze the water sample for tritium. Two 5 ml aliquots of the sample were dispensed into 20 ml plastic scintillation vials with 15 ml of cocktails. The samples with similarly prepared background and quality control samples were counted as a batch three times. Each batch was counted for 300 minutes per cycle. The minimum detectable activity was approximately 4.7 Bq/l.

The tritium in the soil was measured by an outside company [4] which heated a small amount of the irradiated soil $(0.05 - 0.2$ g) to ignition. The combustion gases were condensed, collected in a liquid scintillation vial and counted.

[3] Packard BioSciences, Canberra Industries, 800 Research Parkway, Meriden, CT 06450

[4] Thermo Retec Nuclear Service, 7030 Wright Ave., Richmond, VA 94804

3.2 Gamma Spectroscopy

The gamma rays from the irradiated soil and water samples as well as the metallic disks were measured with a high purity Ge-detector. The spectroscopy of the samples was performed using the EG&G ORTEC Gammavision data acquisition and analysis package [5] . The Gammavision package is comprised of a set of complete algorithms for nuclide identification, background subtraction, efficiency corrections and the determination of the activity for each radionuclide. A sample of the irradiated soil of a weight of 579.9 g was counted for 12 hours.The background was determined by counting an un-irradiated sample of the soil, weighting 582.2 g, in the same geometry. The activity of ^{40}K was measured at 0.42 Bq/g. The activities of ^{232}Th and ^{382}U were estimated from their progenies to be 0.013 and 0.27 Bq/g. The same detector was used to measure the activity of a 480 ml sample of the irradiated water and the metallic disks. The water and the metallic samples were counted for 12 and 4 hours, respectively. A traceable source of the National Institute of Standards and Technology (NIST) was used to create the efficiency and energy calibrations. In addition, a post-measurement comparison of the calibration files to the source was performed as a quality control check.

4 The FLUKA Calculations

The concentration of different radionuclides in the samples was calculated with FLUKA based on a detailed description of the experimental setup. A 13 m long section of the beam tunnel was modelled containing the copper dump and its support structure, the samples, local lead shielding along one side and downstream of the dump and the main beam dump D400 which is a big cylindrical water tank. Fig. 2 shows longitudinal and transverse sections through the geometry of the copper dump and the samples. The D400 dump is downstream of the copper dump and not shown in the figure. The small object in front of the copper-dump (see Fig. 2a) is a strontium-ferrite probe which was installed as part of a material damage study. The bodies to the left of the dump in Fig. 2b) are lead and copper shielding blocks, respectively. The geometry also contained the metallic samples in their true size. The aluminum and copper disks were taped on top of the soil bottle (see Fig. 2b) and the iron disk on top of the water bottle. The origin of the coordinate frame of the FLUKA geometry was chosen to be in the center of the front face of the SrFe probe, the z-axis coinciding with the beam axis and the x-axis pointing up.

The elemental compositions of the samples were defined in the simulations

[5] EG&G Ortec, 100 Midland Road, Oak Ridge, TN 37831

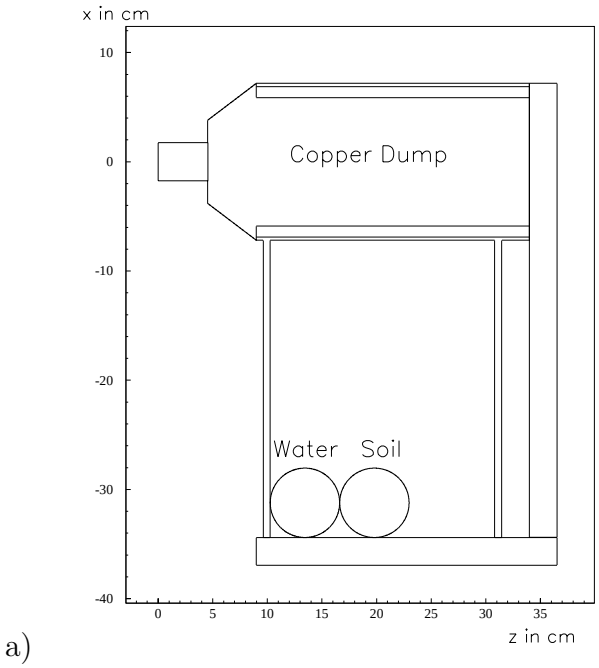

a)

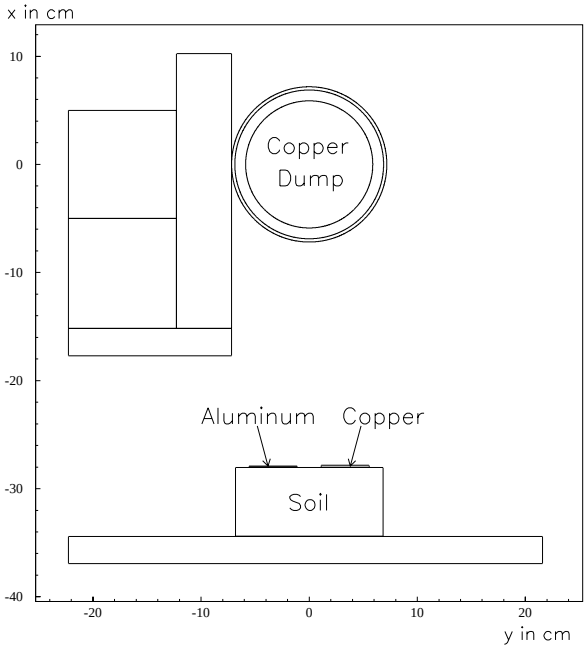

b)

Fig. 2. Sections through the geometry used in the simulations: a) longitudinal section containing the beam axis ($y = 0$) and b) transverse section through the soil bottle and the aluminum and copper disks ($z = 20$ cm).

according to the elemental analyses as listed in Tables 1 and 2. The full electromagnetic and hadronic cascades were simulated in the dump, the samples and the shielding items including particles back-scattered from the main dump and the beam tunnel walls. Electrons and photons were transported down to a kinetic energy of 12 MeV and 10 MeV, respectively, and neutrons down to thermal energies. The former limits are below the threshold for the produc-

tion of the Giant Resonance neutrons in most of the materials. It should be noted that the present FLUKA version uses fits to evaluated experimental cross section data for Giant Resonance interactions up to the mass of copper [9].

In order to increase the statistical significance of the results for the samples (in particular for the thin disks) importance biasing was applied to a region containing both bottles and the three disks. Further biasing techniques used in the simulations include leading particle biasing and inelastic interaction length biasing for photons. The cascades initiated by 3.608×10^8 primary electrons were simulated in a total of 164 FLUKA runs and the average yield of radionuclides was calculated.

Figs. 3 and 4 show the neutron and photon fluence per beam electron for

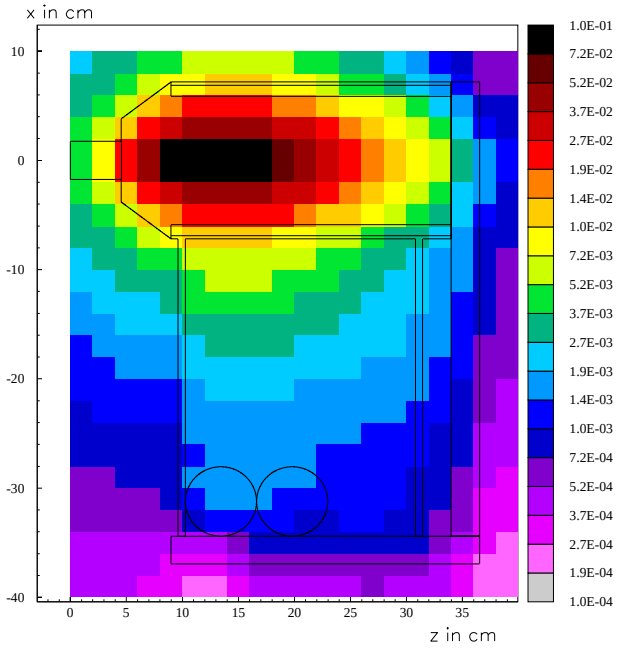

Fig. 3. Neutron fluence per beam electron shown for a longitudinal section through the geometry containing the beam axis. Units are particles/cm^2/electron.

a longitudinal section through the experimental setup containing the beam axis. As can be seen the samples are located in the lateral maximum of the neutron fluence. On the other hand, the electromagnetic cascade is forward-peaked having its lateral maximum downstream of the samples. Note that the fluence-scales are different in Figs. 3 and 4, the photon fluence at the sample locations being about a factor of ten lower than the neutron fluence.

The average neutron energy spectra in the two bottles are shown in Fig. 5. Both spectra are dominated by neutrons of about 1 MeV, the high-energy neutron fluence ($E > 20$ MeV) being almost a factor of 100 lower. The high-energy fluence in the soil is somewhat harder than the one on the water as the soil bottle is located downstream of the water bottle. At low energy the

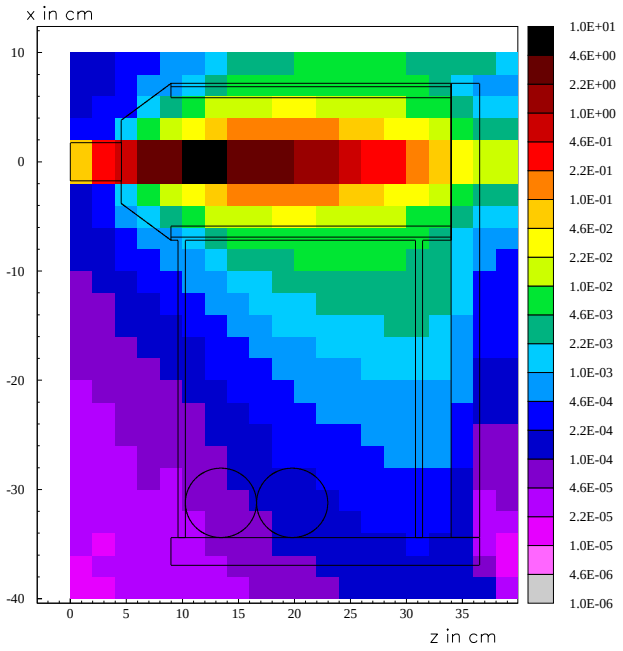

Fig. 4. Photon fluence per beam electron shown for a longitudinal section through the geometry containing the beam axis. Units are particles/cm^2/electron.

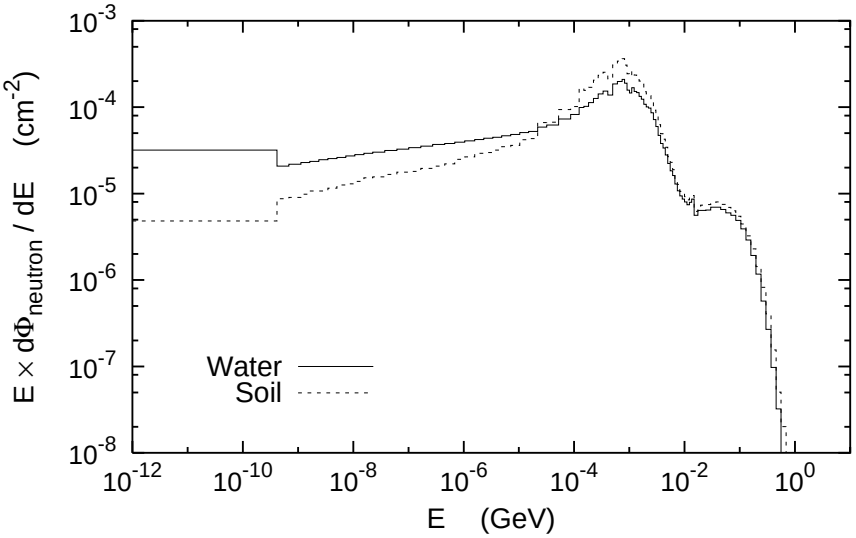

Fig. 5. Average neutron energy spectrum in the water and soil bottles normalized per beam electron.

hydrogen content of water clearly moderates the neutrons resulting in a lower peak at 1 MeV, a less steep decrease with energy and a higher thermal neutron fluence than in the soil bottle. The latter implies that the iron sample which was taped on top of the water bottle was exposed to a much higher thermal neutron fluence than are the other two samples.

In the simulations the total yield of radionuclides and the yield produced by

low-energy neutrons (i.e., below the threshold for the multigroup treatment, $E < 19.6$ MeV) was scored for all samples and the results written into output files. The output from the 164 FLUKA runs was then combined in a post-processing step and the standard deviation calculated for each isotope. Based on these results the specific activity for each isotope was calculated for the time of the data analysis. For example, the metallic samples were analyzed at the end of September, i.e. almost 8 months after the irradiation, and the water and soil samples were analyzed in March and April, respectively. For the decay corrections the actual irradiation profile (see Fig. 1) and the decay channels up to the third generation were taken into account. [6]

5 Results

The results for the soil sample are summarized in Table 3. The isotopes listed

Table 3
Results of experiment and calculations for the specific activity in the soil sample. In the last column the calculated contribution of low-energy neutron interactions to the total isotope production, f_{low} is given.

Isotope	$t_{1/2}$	Experiment (Bq/g)	FLUKA (Bq/g)	Ratio FLUKA/Exp.	f_{low} (%)
^{3}H	12.3 y	$0.313 \pm 15.9\%$	$0.108 \pm 2.8\%$	$0.35 \pm 16.1\%$	0.0
^{7}Be	53.3 d	$2.06 \pm 6.0\%$	$1.23 \pm 3.6\%$	$0.60 \pm 7.0\%$	0.0
^{22}Na	2.6 y	$0.562 \pm 5.9\%$	$0.315 \pm 3.7\%$	$0.56 \pm 7.0\%$	4.4
^{46}Sc	83.8 d	$0.294 \pm 6.0\%$	$0.06 \pm 8.1\%$	$0.20 \pm 10.1\%$	0.0
^{48}V	16.0 d	$0.0279 \pm 6.1\%$	$0.019 \pm 20.2\%$	$0.68 \pm 21.1\%$	0.0
^{51}Cr	27.7 d	$0.872 \pm 6.1\%$	$0.571 \pm 8.7\%$	$0.65 \pm 10.6\%$	44.5
^{54}Mn	312.1 d	$0.549 \pm 6.0\%$	$0.436 \pm 5.4\%$	$0.79 \pm 8.1\%$	30.4
^{59}Fe	44.5 d	$0.0652 \pm 6.3\%$	$0.139 \pm 19.0\%$	$2.1 \pm 20.0\%$	100.0
^{58}Co	70.8 d	$0.0443 \pm 6.1\%$	$0.047 \pm 16.8\%$	$1.1 \pm 17.9\%$	100.0
^{60}Co	5.3 y	$0.0226 \pm 6.1\%$	$9.53 \times 10^{-7} \pm 16.1\%$	$4.2 \times 10^{-5} \pm 17.2\%$	0.0
^{134}Cs	2.1 y	$0.0106 \pm 7.2\%$	–	–	–

are only those which were identified in the experiment. The experimental errors contain both the statistical and systematic uncertainties of the spectroscopy

[6] The decay correction was calculated with a modified version of the `usrsuw`-routine by A. Ferrari

analysis. In case of the calculations the errors represent the standard deviation as mentioned above. In addition to the measured and calculated specific activities their ratio and the percentage contribution of low-energy neutron interactions to the total yield of a particular isotope are given.

More than half of the isotope yields are predicted by FLUKA within 50%. The presence of ^{134}Cs in the measurements indicates that the soil contained elements which were not identified by the elemental analysis. The same argument might also apply to the ^{60}Co-activity which is predicted to be very small, in contrast to the experimental value. As can be seen from the last column in Table 3, ^{59}Fe and ^{58}Co are exclusively produced in low-energy neutron interactions.

The specific activities of ^{3}H and ^{7}Be in the water sample are compared to the FLUKA results in Table 4. The calculated activity of tritium is again

Table 4
As in Table 3, here for the water sample.

Isotope	$t_{1/2}$	Experiment (Bq/g)	FLUKA (Bq/g)	Ratio FLUKA/Exp.	f_{low} (%)
^{3}H	12.3 y	$0.659 \pm 3.1\%$	$0.121 \pm 2.1\%$	$0.18 \pm 3.7\%$	0.0
^{7}Be	53.3 d	$5.67 \pm 6.9\%$	$4.0 \pm 4.0\%$	$0.71 \pm 8.0\%$	0.0

significantly lower than the measured value whereas one would expect a much better agreement as tritium production from light targets is well-predicted in other cases [10].

The specific activities in the metallic samples are summarized in Tables 5 to 7. The presence of the Co-isotopes in the measurements for the iron sample is

Table 5
As in Table 3, here for the iron sample.

Isotope	$t_{1/2}$	Experiment (Bq/g)	FLUKA (Bq/g)	Ratio FLUKA/Exp.	f_{low} (%)
^{46}Sc	83.8 d	$0.282 \pm 7.1\%$	$0.527 \pm 8.4\%$	$1.9 \pm 11.0\%$	0.0
^{51}Cr	27.7 d	$0.443 \pm 32.1\%$	$0.170 \pm 8.4\%$	$0.38 \pm 33.2\%$	0.0
^{54}Mn	312.1 d	$32.9 \pm 6.0\%$	$17.2 \pm 6.2\%$	$0.52 \pm 8.6\%$	27.0
^{59}Fe	44.5 d	$0.550 \pm 6.9\%$	$0.777 \pm 14.8\%$	$1.4 \pm 16.3\%$	100.0
^{58}Co	70.8 d	$0.0663 \pm 24.4\%$	–	–	–
^{60}Co	5.3 y	$0.225 \pm 7.2\%$	–	–	–

Table 6
As in Table 3, here for the aluminum sample.

Isotope	$t_{1/2}$	Experiment (Bq/g)	FLUKA (Bq/g)	Ratio FLUKA/Exp.	f_{low} (%)
^{22}Na	2.6 y	$1.24 \pm 6.6\%$	$0.27 \pm 19.7\%$	$0.22 \pm 20.8\%$	0.0
^{54}Mn	312.1 d	$0.11 \pm 20.3\%$	–	–	–

Table 7
As in Table 3, here for the copper sample.

Isotope	$t_{1/2}$	Experiment (Bq/g)	FLUKA (Bq/g)	Ratio FLUKA/Exp.	f_{low} (%)
^{46}Sc	83.8 d	$0.044 \pm 10.9\%$	$0.106 \pm 7.0\%$	$2.4 \pm 12.9\%$	0.0
^{54}Mn	312.1 d	$0.964 \pm 6.1\%$	$0.498 \pm 15.1\%$	$0.52 \pm 16.3\%$	0.0
^{59}Fe	44.5 d	$0.124 \pm 10.6\%$	$0.034 \pm 24.4\%$	$0.27 \pm 26.6\%$	0.0
^{56}Co	77.3 d	$0.324 \pm 6.5\%$	$0.116 \pm 18.7\%$	$0.36 \pm 19.8\%$	0.0
^{57}Co	271.8 d	$2.02 \pm 6.0\%$	$1.29 \pm 8.7\%$	$0.64 \pm 10.6\%$	0.0
^{58}Co	70.8 d	$3.59 \pm 6.0\%$	$1.93 \pm 4.8\%$	$0.54 \pm 7.7\%$	10.5
^{60}Co	5.3 y	$1.41 \pm 6.0\%$	$0.514 \pm 5.6\%$	$0.36 \pm 8.2\%$	63.0
^{65}Zn	244.3 d	$0.094 \pm 12.0\%$	$0.041 \pm 53.5\%$	$0.44 \pm 54.8\%$	10.5

most likely due to an element which was present in the alloy but not identified in the chemical analysis (such as nickel). Similar arguments may also explain the presence of ^{54}Mn in the analysis of the irradiated aluminum disk. All other isotopes are predicted within about a factor of $2-3$ and are mostly underestimated. A normalization uncertainty as reason for the latter can be excluded since the number of electrons on the dump is relatively well known (to within a few percent). All calculated values with statistical errors larger than about 15%, such as ^{22}Na in the aluminum disk and ^{59}Fe and ^{65}Zn in the copper disk, should be taken with caution as the true uncertainty might be larger than the errors quoted.

6 Discussion and Conclusions

An activation experiment has been performed in the Beam Dump East facility at SLAC during which samples of soil, water, aluminum, copper and iron were irradiated in stray radiation fields generated by interactions of 28.5 GeV electrons in a copper dump. Prior to the experiment the chemical composition

of the samples was determined. The specific activities were measured using various techniques, such as gamma spectroscopy. In addition, the experiment was simulated in detail using the FLUKA code.

The comparison of measured and calculated activities showed that the isotope yields are underestimated by the calculations, in most cases by about a factor of 2, in some cases by up to a factor of $3 - 5$. In order to understand and evaluate these results it must be noted that the radiation field causing induced radioactivity at electron accelerators is very complex as it involves both electromagnetic and hadronic processes - a situation which is different from that found at proton accelerators. Therefore, also the reasons for the discrepancies between measured and calculated activities are of complex nature. The experimental uncertainties include the following:

- There are statistical and systematic uncertainties in the spectroscopy methods used to analyze the irradiated samples. These include calibration uncertainties, such as possible differences in self absorption in the samples with respect to calibration sources (self-absorption corrections become large in relatively thick samples) and uncertainties in energy calibration. In addition, uncertainties associated with background subtraction could cause significant difficulties in correctly identifying the radionuclides and their intensities in different samples. All these uncertainties are reflected in the errors quoted for the measured activities in Tables 3 to 7.
- The overall normalization of the measured activation depends on the total number of beam particles on the target. Any uncertainty leads to an offset between the measured and calculated yields. In addition, for long irradiations and/or relatively short-lived isotopes an accurate consideration of the beam pattern is essential. In the present experiment both uncertainties are relatively small.
- In order to simulate the experiment with a Monte Carlo code the elemental composition of the samples has to be determined. The presence of trace amounts of some elements not identified in the elemental analysis may cause significant discrepancies between measured and calculated activities of certain isotopes. For example, the presence of ^{134}Cs in the spectroscopy results for soil, the presence of the cobalt isotopes in the results for iron and of ^{54}Mn in the results for aluminum suggests deficiencies in the elemental analysis determining the composition of the samples.

On the other hand, the following uncertainties in the Monte Carlo simulations and models may contribute to the observed discrepancies:

- Predictions for isotopes produced by thermal neutron capture depend strongly on the accurate description of moderating materials in the vicinity of the experiment, such as concrete walls, the huge water dump or the water bottle in the present study. If these factors are neglected or modelled incompletely

the predictions for those isotopes can well be off by large factors. However, in the present study the material distribution around the experiment has been modelled rather accurately. In addition, these isotopes are not produced at all if the code does not contain the corresponding cross section information, such is the case for Zn, Ga, Br and Sr in FLUKA.

- The small size of the metallic samples causes large statistical uncertainties which can not be compensated by increasing the computing time. Calculated activities carrying statistical uncertainties larger than about 20% cannot be considered to be reliable. Unfortunately, the size effect on the theoretical uncertainties is opposite to the one on the experimental uncertainties where thick samples result in large self-absorption corrections (see above). It would be desirable to have the option of biasing the production of residual nuclei in the Monte Carlo code, such as repeated sampling of an inelastic interaction and adjusting (reducing) the weight of the interaction correspondingly.
- The description of isotope production by integrated Monte Carlo transport codes is based on many different models for both transport and interactions of particles. The particle which eventually creates the isotope is often of high generation in the "tree" of the cascade (especially in activation by stray radiation fields). Small inaccuracies at each interaction or transport step can thus add up to sizeable uncertainties in the predictions for a certain isotope and it is often difficult to trace back the reason to a specific model. For example, the simulation of Giant Dipole Resonance (GDR) interactions is based on evaluated experimental cross sections. These cross sections often carry up to a factor of two uncertainty. Therefore, also the neutron field produced by GDR interactions and the isotopes produced in re-interactions of these neutrons (or produced directly in the GDR interaction) is modelled only within the same uncertainty. In this respect, integrated codes, such as FLUKA, should be preferred to multi-step simulations where the output of one code (such as photon tracklengths) is used as input for a second code (for example to simulate the photonuclear interaction) as those interfaces often cause additional uncertainties.

Taking these uncertainties into account the agreement of measured and calculated induced radioactivity within a factor of two, as is the case for half of the identified isotopes in this study, can be considered to be acceptable. However, the uncertainties together with the scarcity of experimental information on induced radioactivity at electron accelerators clearly calls for further measurements as benchmark for Monte Carlo transport codes.

Acknowledgments

We would like to thank Ronald Seefred and Roger Sit for their assistance during the measurements and Paola Sala for valuable comments on the manuscript.

This work was supported by the Department of Energy contract DE-AC03-76SF00515.

References

[1] P. Swanson, Radiological safety aspects of the operation of electron linear accelerators. Technical Report Series no. 188 (IAEA, Ed.) Vienna (1979).

[2] A. Fassò, M. Silari and L. Ulrici, Predicting induced radioactivity at high-energy electron accelerators. In *Proceedings of the Ninth International Conference on Radiation Shielding, ICRS-9*, Tsukuba, Japan, 1999, *Journal of Nuclear Science and Technology*, Suppl. **1**, 827 (2000).

[3] A. Fassò, A. Ferrari, J. Ranft and P. R. Sala, New developments in FLUKA modeling of hadronic and EM interactions. In *Proceedings of The Third Workshop on Simulating Accelerator Radiation Environments (SARE-3)* (H. Hirayama, Ed.), pp. 32-43, Proceedings 97-5, KEK, Tsukuba, Japan, 1997.

[4] A. Fassò, A. Ferrari and P. R. Sala, Electron-photon transport in FLUKA: Status. To appear in *Proceedings of the International Conference on Advanced Monte Carlo for Radiation Physics, Particle Transport Simulation and Applications, Monte Carlo 2000* (P. Vaz, Ed.), Lisbon, Portugal, 2000.

[5] A. Fassò, A. Ferrari, J. Ranft and P. R. Sala, FLUKA: Status and perspectives for hadronic applications. To appear in *Proceedings of the International Conference on Advanced Monte Carlo for Radiation Physics, Particle Transport Simulation and Applications, Monte Carlo 2000* (P. Vaz, Ed.), Lisbon, Portugal, 2000.

[6] M. Silari, L. Ulrici and S. Ye, On the estimation of low levels of induced radioactivity in LEP. CERN Internal Report, TIS-RP/IR/99-13, 1999.

[7] S. Rokni, J. C. Liu and S. Roesler, Initial Estimates of the Activation Concentration of the Soil and Groundwater around the NLC Beam Delivery System Tunnel. In *Proceedings of the Fifth Specialists Meeting on Shielding Aspects of Accelerators, Targets and Irradiation Facilities (SATIF-5)*, Paris, France, 2000, Proceedings OECD-NEA, p. 115, 2001.

[8] S. Ban, H. Nakamura, T. Sato and K. Shin, *Radiat. Prot. Dosim.* **93**, 231 (2000).

[9] A. Fassò, A. Ferrari and P. R. Sala, Total Giant Resonance photonuclear cross sections for light nuclei: A database for the FLUKA Monte Carlo transport code. In *Proceedings of The Third Specialists Meeting on Shielding Aspects of Accelerators, Targets and Irradiation Facilities (SATIF-3)*, Tohoku University, Sendai, Japan, 1997, Proceedings OECD-NEA, pp. 61-74, 1998.

[10] A. Ferrari, and P. R. Sala, Intermediate and high energy models in FLUKA: improvements, benchmarks and applications. In *Proceedings of the*

International Conference on Nuclear Data for Science and Technology, NDST-97 (G. Reffo, A. Ventura and C. Grandi, Eds.), Trieste, Italy, 1997, p. 247, 1997.